

1 Magma hybridisation and diffusive exchange recorded in heterogeneous  
2 glasses from Soufrière Hills Volcano, Montserrat

3

4 Humphreys, M.C.S.<sup>1\*</sup>, Edmonds, M.<sup>1,2</sup> Christopher, T.<sup>3</sup> & Hards, V.<sup>4</sup>

5 <sup>1</sup> Department of Earth Sciences, University of Cambridge, Downing Street, Cambridge, CB2 3EQ, UK

6 <sup>2</sup> COMET+, National Centre for Earth Observation

7 <sup>3</sup> Montserrat Volcano Observatory, Flemmings, Montserrat, West Indies

8 <sup>4</sup> British Geological Survey, Keyworth, Nottingham, NG12 5GG

9

10 \* Corresponding author: Tel: +44 (0)1223 333433; Email: mcsh2@cam.ac.uk

11

12 Running title: Magma hybridisation at Soufrière Hills Volcano

13

14

15

Special issue: Montserrat - CALIPSO

16

17

18

### ABSTRACT

19 Arc volcanoes commonly show evidence of mixing between mafic and silicic magma.

20 Melt inclusions and matrix glasses in andesite erupted from Soufrière Hills Volcano

21 include an anomalously K<sub>2</sub>O-rich population which shows close compositional

22 overlap with residual glass from mafic inclusions. We suggest that these glasses

23 represent the effects of physical mixing with mafic magma, either during ascent or by

24 diffusive exchange during the formation of mafic inclusions. Many glasses are

25 enriched only in K<sub>2</sub>O, suggesting diffusive contamination by high-K mafic inclusion

26 glass; others are also enriched in TiO<sub>2</sub>, suggesting physical mixing of remnant glass.

27 Some mafic inclusion glasses have lost K<sub>2</sub>O. The preservation of this K-rich melt

28 component in the andesite suggests short timescales between mixing and ascent.

29 Diffusive timescales are consistent with independent petrological estimates of magma

30 ascent time.

31

32

### INTRODUCTION

33 Many arc volcanoes are dominated by interaction between mafic and silicic magmas.

34 Recharge by hotter, more mafic material is frequently cited as an eruption trigger, and

35 transfer of volatiles may be important in both promoting mixing (e.g. *Eichelberger*,  
36 1980) and advecting heat into, and remobilising, the overlying crystal-rich silicic  
37 magma (*Bachmann and Bergantz*, 2006). Magma mingling (incomplete mixing)  
38 produces quenched magmatic enclaves, crystal clusters and other clear disequilibrium  
39 textures (*Anderson*, 1976; *Bacon*, 1986; *Clyne*, 1999). Recognising the products of  
40 magma *hybridisation* (complete mixing) is important for understanding the relative  
41 proportions and compositions of the end-member magmas, the likely impact of  
42 repeated recharge, and the processes causing mass transfer between magmas.

43

44 Recent studies have shown that microlites of anomalously An-rich plagioclase (as  
45 well as clinopyroxene and Mg-rich orthopyroxene) in intermediate arc magmas  
46 originate in mafic magmatic enclaves or ‘mafic inclusions’ (*Martel et al.*, 2006;  
47 *Humphreys et al.*, 2009a). The microlites are transferred into the andesite either  
48 during mixing in the chamber (*Martel et al.* 2006) or by physical break-up and  
49 disaggregation of mafic inclusions by shearing during ascent (*Humphreys et al.*,  
50 2009a). This physical transfer of crystals will increase magma viscosity in the conduit  
51 and therefore has implications for eruption dynamics, as well as the potential to be  
52 used as a tracer of the mafic component. With effective mixing, one might also expect  
53 to see a mafic melt component. Melt inclusions and matrix glasses are commonly  
54 used to track magma evolution paths and assess magma storage conditions (e.g.  
55 *Sisson and Layne*, 1993; *Wallace et al.*, 1995; *Blundy et al.*, 2006), so it is vital to  
56 determine whether melt derived from the mafic magma is entering the andesite, and if  
57 so, in what proportions and with what chemical signature. Quantifying the extent and  
58 timescale of interaction between andesitic and mafic magma, which is thought to  
59 drive the eruption, would also be invaluable for volcano monitoring and hazard  
60 assessment. Here we examine evidence that magma mingling *does* involve transfer of  
61 mafic-derived melt, preserved as heterogeneity in plagioclase-hosted melt inclusions  
62 and matrix glasses.

63

## 64 **GEOLOGICAL BACKGROUND AND SAMPLES STUDIED**

65 The Soufrière Hills Volcano on Montserrat lies in the Lesser Antilles subduction zone  
66 and has been active for approximately ~300 ka (*Harford et al.*, 2002). The most  
67 recent eruption started in 1995, with a series of pulses of dome growth and explosive  
68 activity, interrupted by long pauses when no magma was erupted. Major dome

69 collapses occurred in December 1997, July 1999, July 2001, July 2003 and May 2006.  
70 Currently (September 2009) activity is limited to low-level residual activity, although  
71 with continuing significant gas emissions ([www.mvo.ms](http://www.mvo.ms)).

72

73 Products from the current eruption are porphyritic andesite, with phenocrysts of  
74 hornblende, plagioclase, orthopyroxene and Fe-Ti oxides plus rhyolite glass or  
75 groundmass. Disequilibrium crystal textures are common, including rare, resorbed  
76 quartz phenocrysts, oscillatory zoning in plagioclase and hornblende, reversely zoned  
77 orthopyroxene and sieve-textured plagioclase (*Murphy et al.*, 2000). The groundmass  
78 contains microlites of plagioclase, orthopyroxene, clinopyroxene and Fe-Ti oxides as  
79 well as rhyolitic glass, and may show extensive crystallisation, incipient  
80 devitrification and deposits of cristobalite. Macroscopic mafic inclusions have been  
81 described in detail (*Murphy et al.*, 1998; 2000) and contain plagioclase,  
82 clinopyroxene, orthopyroxene, Fe-Ti oxides and rhyolitic interstitial glass; larger  
83 inclusions also crystallise pargasitic amphibole (*Murphy et al.*, 1998). Many of the  
84 microlites in the andesite are derived from mafic inclusions, as are crystal clusters, i.e.  
85 mafic-derived fragments that can be recognised by texture and mineral compositions  
86 (*Humphreys et al.*, 2009a).

87

88

## RESULTS

89 We analysed plagioclase-hosted melt inclusions, matrix glass and residual mafic  
90 inclusion glass from 23 samples erupted between July 2001 and July 2008 (see  
91 supplementary table 1). Most of the samples represent typical andesite. Sample  
92 MVO1532d is a heterogeneous mixture of nearly microlite-free rhyolite glass  
93 containing euhedral quartz, plagioclase and hornblende, with fine-grained, crystal-rich  
94 patches with very little remaining glass. Sample preparation and analytical methods,  
95 together with the procedure used to correct for post-entrapment crystallisation (PEC)  
96 of melt inclusions, are described in the auxiliary material.

97

### Melt inclusions

99 Melt inclusions are rhyolitic, with 71-79 wt% SiO<sub>2</sub> (see supplementary data table 2;  
100 figures show PEC-corrected values, normalised to 100% anhydrous). Compositions  
101 are similar to those reported by *Edmonds et al.* (2001), *Harford et al.* (2003) and  
102 *Buckley et al.* (2006). Two populations can be distinguished on the basis of K<sub>2</sub>O

103 contents (figure 1). Most inclusions have 2–3 wt% K<sub>2</sub>O, increasing with SiO<sub>2</sub> and Cl  
104 contents, but a minority of inclusions has up to 6 wt% K<sub>2</sub>O. For the low-K population,  
105 Al<sub>2</sub>O<sub>3</sub>, CaO and Na<sub>2</sub>O show a scattered negative relationship with SiO<sub>2</sub>. FeO, MgO  
106 and TiO<sub>2</sub> subtly increase with SiO<sub>2</sub>, and also correlate with each other (e.g. figure 1d).  
107 The high-K inclusion population has lower CaO than the low-K glasses, and slightly  
108 lower Cl (figure 1). Two inclusions have high TiO<sub>2</sub> but low K<sub>2</sub>O (figure 2). High-K  
109 glasses were not present in pumiceous samples.

110

### 111 **Matrix glasses**

112 Matrix glass was analysed in samples without significant groundmass crystallisation  
113 (supplementary table 1). Matrix glasses are rhyolitic, clustering at the SiO<sub>2</sub>-rich end of  
114 the melt inclusion trends (75-79 wt% SiO<sub>2</sub>, figure 1). There are four groups of matrix  
115 glasses: (i) high-K, low-Ti, (ii) low-K, low-Ti, (iii) high-K, high-Ti, and (iii) low-K,  
116 high-Ti compositions (figure 2). High-K matrix glasses extend to lower CaO contents  
117 than low-K glasses (figure 1b). Some glasses have anomalously low MgO. High-K  
118 glasses were not present in the pumice samples.

119

### 120 **Mafic inclusion glass**

121 Residual mafic inclusion glasses are also rhyolitic (72-78 wt% SiO<sub>2</sub>). In Si, Al, Fe and  
122 Na composition they are indistinguishable from the melt inclusions. However, they  
123 have distinctive high-Ti, high-K compositions (figure 2) and also show low CaO  
124 contents, similar to the other high-K glasses. Many of the residual glasses also have  
125 low MgO contents. Cl concentrations are variable but tend to be lower than in the  
126 melt inclusions (figure 1).

127

128

## DISCUSSION

129 In general, the negative correlations of Al<sub>2</sub>O<sub>3</sub>, CaO and Na<sub>2</sub>O with SiO<sub>2</sub> in the melt  
130 inclusions indicate decompression crystallisation dominated by plagioclase (e.g.  
131 *Buckley et al.*, 2006). The positive correlation between FeO and MgO, and slight  
132 increase of both MgO and FeO with SiO<sub>2</sub> suggests minor crystallisation of  
133 orthopyroxene or hornblende as observed in the andesite. Ti-Fe variations are  
134 consistent with crystallisation of minor Ti-magnetite. The low-K matrix glasses  
135 follow mainly the same compositional trends as the low-K melt inclusions but tend  
136 towards higher K<sub>2</sub>O and higher SiO<sub>2</sub>, as K is enriched in the melt during groundmass

137 crystallisation (*Harford et al.*, 2003). Low-K matrix glasses show decreasing MgO  
138 with increasing SiO<sub>2</sub>, consistent with groundmass crystallisation of orthopyroxene.  
139 The trend of decreasing Cl with increasing K<sub>2</sub>O in the matrix glass (figure 1f)  
140 indicates degassing of Cl during decompression crystallisation (*Edmonds et al.*, 2001;  
141 *Harford et al.*, 2003; *Humphreys et al.*, 2009b).

142 The low-Ca, low-Mg compositions of the mafic inclusion residual glasses are  
143 consistent with significant crystallisation of clinopyroxene in the mafic inclusions.  
144 The very high K<sub>2</sub>O contents of mafic inclusion glasses are consistent with the lower  
145 proportions of amphibole in the mafic inclusions and their lower bulk SiO<sub>2</sub> contents  
146 relative to the andesite; their high TiO<sub>2</sub> may be related to the high TiO<sub>2</sub> of the bulk  
147 mafic inclusions.

148

#### 149 **Origin of high-K glass**

150 While the main compositional characteristics of the glass suite are consistent with  
151 near-surface processes (see above), the K-rich signature of some glasses is not. The  
152 occasional high TiO<sub>2</sub>, high-K<sub>2</sub>O, low MgO and low CaO contents are also seen in  
153 previously reported matrix glasses (*Edmonds et al.*, 2001; 2002; *Harford et al.*, 2003;  
154 *Buckley et al.*, 2006; see figure 1). These compositional features are largely shared by  
155 the residual mafic inclusion glasses.

156 The anomalous glass compositions cannot be caused by boundary layer effects  
157 during melt inclusion entrapment (*Baker*, 2008) because only slowly diffusing  
158 incompatible elements should be enriched in the melt boundary layer, whereas K<sup>+</sup>  
159 diffusivities are rapid (*Jambon*, 1983). Similarly, post-entrapment crystallisation of  
160 host plagioclase should result in coupled increases of MgO, TiO<sub>2</sub> and K<sub>2</sub>O with  
161 decreasing CaO, which are not observed, and cannot account for anomalous matrix  
162 glass compositions.

163 K-rich glasses or crystalline products have been ascribed to grain-boundary  
164 partial melting of mafic cumulate nodules (*Dungan and Davidson*, 2004; *Heliker*,  
165 1995) or assimilation of biotite-rich cumulates (*Reubi and Blundy*, 2008), with K-rich  
166 and host melts mixing during subsequent nodule break-up. However, cumulate  
167 nodules are relatively rare in Soufrière Hills andesite and were not observed in any of  
168 the samples studied, while the high-K glasses are texturally indistinguishable from  
169 ‘normal’ glasses and their host crystals are not obviously xenocrystic. Finally, K-rich

170 glasses are also found in mafic inclusions, which are widely agreed to form by rapid  
171 quenching against a cooler host (*e.g. Wager and Bailey 1953; Yoder 1973*).  
172 *Buckley et al. (2006)* ascribed the high-K compositions to hornblende  
173 breakdown during slow magma ascent and mixing between more- and less-evolved  
174 melts. Mass balance between the dissolving hornblende and the observed rims (cpx +  
175 opx + plag + oxides) indicated that melts modified by hornblende breakdown should  
176 thus be compositionally variable, with high TiO<sub>2</sub> and MgO but low SiO<sub>2</sub> and FeO.  
177 The melts should all have high K<sub>2</sub>O, Na<sub>2</sub>O and Cl (*Buckley et al., 2006*). Neither of  
178 their predicted trends fits with all the observed compositional variations (figure 1).  
179 Interstitial melts in hornblende breakdown rims (*Buckley et al., 2006*) actually show  
180 *both* high-K and low-K compositions (figure 1a), not just high-K compositions as  
181 expected. We therefore conclude that decompression breakdown of hornblende cannot  
182 adequately describe the high-K glasses.

183

#### 184 **Magma hybridisation and diffusive contamination**

185 We propose that the K-rich melts are derived from, or affected by mixing with  
186 intruding mafic magma. The K-rich compositions are similar to those of mafic  
187 inclusion residual glass, and incorporation of K-rich melt into the host matrix is  
188 consistent with transfer of microlites into the andesite groundmass by disaggregation  
189 of mafic inclusions (*Humphreys et al., 2009a*). However, K<sub>2</sub>O-TiO<sub>2</sub> concentrations  
190 demonstrate the presence of four distinct glass compositions (see earlier; figure 2): (i)  
191 low-K, low-Ti; (ii) low-K, high-Ti; (iii) high-K, high-Ti; and (iv) high-K, low-Ti.  
192 This indicates that the mafic inclusion glasses are, for the most part, not being  
193 transferred unmodified into the host andesite, and suggests diffusive modification.  
194 Breaking open partially crystalline mafic inclusions would allow interaction between  
195 host (rhyolite) melt from the andesite and residual rhyolite from the interior of the  
196 mafic inclusions. Similarly, complete disaggregation of mafic inclusions would result  
197 in physical transfer of K-rich, Ti-rich residual rhyolite, which can be modified by  
198 diffusive re-equilibration with the host melt. Diffusion of TiO<sub>2</sub> is much slower than  
199 that of K<sub>2</sub>O (see later), so residual mafic glass that has lost K<sub>2</sub>O by diffusion still  
200 retains its high-Ti signature, whereas the high-K host rhyolite cannot gain TiO<sub>2</sub> by  
201 diffusion (figure 2). The result is anomalously K-rich (but Ti-poor) host rhyolite melt,  
202 and K-poor (but Ti-rich) residual mafic inclusion glasses. This process explains the  
203 lack of ubiquitous Ti-enrichment of high-K melt inclusions and matrix glasses

204 compared with mafic inclusion glass. Once a pocket of K-rich melt is present in the  
205 matrix of the andesite, it can be incorporated into melt inclusions by sealing of proto-  
206 inclusions during ascent-driven crystallisation (see *Humphreys et al.*, 2008, figure 11).

207

### 208 **Timescales of between mixing and eruption**

209 The glass compositions and distribution can give further insight into the physical  
210 processes involved in transfer of material. For example, the lack of K-rich glasses in  
211 pumiceous samples (see earlier) implies that K-enrichment occurs during slow ascent.  
212 Many of the K-rich compositions are matrix glass, with relatively few high-K melt  
213 inclusions. This also suggests that transfer occurs primarily during low-pressure  
214 ascent and crystallisation, and could be explained by lower shear stresses in the  
215 conduit during rapid ascent of less viscous, less crystalline magma (e.g. *Melnik and*  
216 *Sparks* 2005) compared with the highly viscous, strongly crystalline magma that  
217 erupts slowly during dome growth.

218       Elemental diffusivities can be used to assess the timescales of this process  
219 (*Sparks et al.* 1977; *Baker*, 1991). Alkali and alkaline earth diffusivities ( $D$ ) in  
220 anhydrous rhyolite are  $D_{\text{Na}} \sim 1.6 \times 10^{-6} \text{ cm}^2/\text{s}$ ,  $D_{\text{K}} \sim 8.9 \times 10^{-8} \text{ cm}^2/\text{s}$ , and  $D_{\text{Ca}} \sim 4.0 \times 10^{-10}$   
221  $\text{cm}^2/\text{s}$  at 900 °C (*Jambon* 1983). A first-order approximation of timescales ( $t$ ) can  
222 be made, ignoring the effects of possible differences in melt H<sub>2</sub>O content, from  $x \sim$   
223  $2\sqrt{(Dt)}$ , where  $x$  is the diffusion lengthscale, here taken to be 1 cm. Diffusive  
224 timescales are 43 hours (Na<sup>+</sup>), 32 days (K<sup>+</sup>) and 20 years (Ca<sup>2+</sup>). In other words,  
225 alkaline earth diffusion is slow relative to alkalis; diffusion of highly charged ions  
226 (e.g. Ti<sup>4+</sup>) should be even slower than the alkaline earths (*Henderson et al.* 1985).  
227 Diffusive contamination of alkalis should therefore be rapid, but modification of other  
228 elements would be prohibitively slow (*Baker*, 1991). The K-enrichment of the  
229 rhyolite matrix of the host andesite must therefore have occurred ~1 month or less  
230 prior to eruption of the magma at the surface, in order to preserve the high-K  
231 signature. This is consistent with timescales estimated by preservation of Fe-Ti oxide  
232 zoning (*Devine et al.* 2003) and decompression breakdown rims on hornblende  
233 (*Rutherford and Devine* 2003). The few high-Ti, low-K glasses, and the wide range of  
234 K<sub>2</sub>O contents of residual mafic inclusion glasses (figure 2) may reflect a spread to  
235 longer timescales, allowing complete or partial re-equilibration of K<sub>2</sub>O with the host  
236 rhyolite. We also note that the K<sub>2</sub>O contents of mafic inclusion and high-K host melts

237 are similar, whereas a diffusion couple should give slightly lower  $K_2O$  contents in the  
238 host melt. There are two possible explanations for this: (i) the mafic inclusion glasses  
239 are already diffused and their observed compositions are not primary, or (ii) the high  
240  $K_2O$  in the host rhyolite represents an uphill diffusion ‘spike’ similar to that observed  
241 in experimental diffusion couples (*Bindeman and Davis 1999; van der Laan et al.*  
242 1994). In either case, this observation reinforces the short timescales between mixing  
243 and eruption.

244 The estimated diffusion timescales also suggest that  $Na_2O$  contents would  
245 quickly be homogenised by diffusion between host andesite and mafic inclusions,  
246 while original  $CaO$  contents should be preserved. We would also anticipate rapid  
247 diffusion of volatiles (e.g.  $CO_2$  and  $H_2O$ ), particularly in more  $H_2O$ -rich melt (*Baker*  
248 *et al. 2005*). It is difficult to assess the effects of mixing and diffusion on Ca and Na  
249 as these elements are compatible in the crystallising assemblage and therefore  
250 strongly affected by fractionation of plagioclase, whereas K is strongly incompatible.  
251 However, the K-enriched glasses are slightly depleted in  $CaO$  relative to the normal  
252 glasses, as is the mafic inclusion residual glass. The different diffusivities of  $CaO$  and  
253  $K_2O$  are not consistent with diffusive contamination of both elements: timescales long  
254 enough for significant Ca diffusion would also eliminate any  $K_2O$  signature. The  
255 lower  $CaO$  contents cannot be produced by crystallisation of quartz, or diffusion  
256 gradients around growing plagioclase or pyroxene grains, as discussed earlier. We  
257 suggest that the lower  $CaO$  might be related to continued crystallisation of  
258 plagioclase.

259

260

## CONCLUSIONS

261 Glass compositional heterogeneity from Soufrière Hills Volcano, Montserrat, is  
262 interpreted as the result of mingling between hotter, mafic magma and the host  
263 andesite. High- $K_2O$  melt inclusions and matrix glasses in the andesite overlap with  
264 the compositions of residual glass from mafic inclusions. However,  $K_2O$  and  $TiO_2$   
265 contents are decoupled: many high-K melt inclusions do not show high Ti as seen in  
266 residual mafic inclusion glasses. This can be explained by diffusive exchange between  
267 disaggregated mafic inclusion melt and host matrix melt. The host rhyolite gains  $K_2O$   
268 from mafic inclusions, but the original low  $TiO_2$  contents are unchanged. Conversely,  
269 high-Ti glasses with normal  $K_2O$  contents probably represent residual mafic inclusion  
270 glass that has lost  $K_2O$  by diffusion. The preservation of such heterogeneity can be



271 used to estimate the timescales between mingling and magma ascent to the surface.  
272 The timescales necessary to preserve K heterogeneity are on the order of a month,  
273 which is consistent with magma ascent times estimated from hornblende breakdown  
274 and Fe-Ti oxides.

275

276

#### ACKNOWLEDGEMENTS

277 MCSH acknowledges a Junior Research Fellowship from Trinity College, Cambridge.  
278 ME acknowledges the NERC National Centre for Earth Observation (Theme 6:  
279 Dynamic Earth) grant NE/F001487/1. VH publishes with the permission of the  
280 Executive Director of the British Geological Survey (NERC). This work was partly  
281 supported by the British Geological Survey. We thank Chiara Petrone for assistance  
282 with electron microprobe analysis.

283

284

#### REFERENCES

285 Anderson, A.T. (1976). Magma mixing: Petrological process and volcanological tool.  
286 *J Volcanol Geotherm Res* **1**, 3-33

287

288 Bachmann, O. & Bergantz, G.W. (2006). Gas percolation in upper-crustal silicic  
289 mushes as a mechanism for upward heat advection and rejuvenation of near-solidus  
290 magma bodies. *J Volcanol Geotherm Res* **149**, 85-102

291

292 Bacon, C.R. (1986). Magmatic inclusions in silicic and intermediate volcanic rocks.  
293 *Journal of Geophysical Research* **91**, 6091-6112

294

295 Baker, D.R. (1991). Interdiffusion of hydrous dacitic and rhyolitic melts and the  
296 efficacy of rhyolite contamination of dacitic enclaves. *Contrib Mineral Petrol* **106**,  
297 462-473

298

299 Baker, D.R., Freda, C., Brooker, R.A. & Scarlato, P. (2005). Volatile diffusion in  
300 silicate melts and its effects on melt inclusions. *Annals Geophys* **48**, 699-717

301

302 Baker, D.R. (2008). The fidelity of melt inclusions as records of melt composition.  
303 *Contrib Mineral Petrol* **156**, 377-395

304

305 Bindeman, I.N. & Davis, A.M. (1999). Convection and redistribution of alkalis and  
306 trace elements during the mingling of basaltic and rhyolite melts. *Petrology* **7**, 91-101

307

308 Blundy, J., Cashman, K & Humphreys, M. (2006). Magma heating by decompression-  
309 driven crystallization beneath andesite volcanoes. *Nature* **443**, 76-80

310

311 Buckley, V.J.E., Sparks, R.S.J. & Wood, B.J. (2006). Hornblende dehydration  
312 reactions during magma ascent at Soufrière Hills Volcano, Montserrat. *Contrib*  
313 *Mineral Petrol* **151**, 121-140

314  
315 Clynne, M.A. (1999). A complex magma mixing origin for rocks erupted in 1915,  
316 Lassen Peak, California. *J Petrol* **40**, 105-132  
317  
318 Devine, J.D., Gardner, J.E., Brack, H.P., Layne, G.D. & Rutherford, M.J. (1995).  
319 Comparison of microanalytical methods for estimating H<sub>2</sub>O contents of silicic  
320 volcanic glasses. *Amer Mineral* **80**, 319-328  
321  
322 Devine, J.D., Rutherford, M.J., Norton, G.E. & Young, S.R. (2003). Magma storage  
323 region processes inferred from geochemistry of Fe-Ti oxides in andesitic magma,  
324 Soufrière Hills Volcano, Montserrat, W.I.. *Journal of Petrology* **44**, 1375-1400  
325  
326 Dungan, M.A. & Davidson, J. (2004). Partial assimilative recycling of the mafic  
327 plutonic roots of arc volcanoes: An example from the Chilean Andes. *Geology* **32**,  
328 773-776  
329  
330 Edmonds, M.E., Pyle, D. & Oppenheimer, C. (2001). A model for degassing at the  
331 Soufrière Hills Volcano, Montserrat, West Indies, based on geochemical data. *Earth*  
332 *Plan Sci Lett* **186**, 159-173  
333  
334 Edmonds, M., Pyle, D. & Oppenheimer, C. (2002). HCl emissions at Soufrière Hills  
335 Volcano, Montserrat, West Indies, during a second phase of dome building:  
336 November 1999 to October 2000. *Bull Volcanol* **64**, 21-30  
337  
338 Eichelberger, J.C. (1980). Vesiculation of mafic magma during replenishment of  
339 silicic magma reservoirs. *Nature* **288**, 446-450  
340  
341 Harford, C.L., Pringle, M.S., Sparks, R.S.J. & Young, S.R. (2002). *In* The Eruption of  
342 the Soufrière Hills Volcano, Montserrat, from 1995 to 1999. T. H. Druitt, B. P.  
343 Kokelaar, Eds. (Geological Society Memoir, London, 2002), vol. 21, pp. 93-113.  
344  
345 Harford, C.L., Sparks, R.S.J. & Fallick, A.E. (2003). Degassing at the Soufrière Hills  
346 Volcano, Montserrat, recorded in matrix glass compositions. *J Petrol* **44**, 1503-1523  
347  
348 Heliker, C. (1995). Inclusions in Mount St. Helens dacite erupted from 1980 through  
349 1983. *J Volcanol Geotherm Res* **66**, 115-135  
350  
351 Henderson, P., Nolan, J., Cunningham, G.C. & Lowry, R.K. (1985). Structural  
352 controls and mechanisms of diffusion in natural silicate melts. *Contrib Mineral Petrol*  
353 **89**, 263-272  
354  
355 Humphreys, M.C.S., Kearns, S.L. & Blundy, J.D. (2006). SIMS investigation of  
356 electron-beam damage to hydrous, rhyolitic glasses: Implications for melt inclusion  
357 analysis. *Amer Mineral* **91**, 667-679  
358  
359 Humphreys, M.C.S., Blundy, J.D. & Sparks, R.S.J. (2008). Shallow-level  
360 decompression crystallisation and deep magma supply at Shiveluch Volcano. *Contrib*  
361 *Mineral Petrol* **155**, 45-61  
362

363 Humphreys, M.C.S., Christopher, T. & Hards, V. (2009a). Microlite transfer by  
364 disaggregation of mafic inclusions following magma mixing at Soufrière Hills  
365 volcano, Montserrat. *Contrib Mineral Petrol* **157**, 609-624  
366

367 Humphreys, M.C.S., Edmonds, M., Christopher, T. & Hards, V. (2009b). Chlorine  
368 variations in the magma of Soufrière Hills Volcano, Montserrat: Insights from Cl in  
369 hornblende and melt inclusions. *Geochim Cosmochim Acta* **73**, 5693-5708  
370

371 Jambon, A. (1983). Diffusion dans les silicates fondues: un bilan des connaissances  
372 actualles. *Bull Mineral* **106**, 229-246  
373

374 Martel, C., Radadi Ali, A., Poussineau, S., Gourgaud, A. & Pichavant, M. (2006).  
375 Basalt-inherited microlites in silicic magmas: Evidence from Mount Pelée  
376 (Martinique, French West Indies). *Geology* **34**, 905-908  
377

378 Melnik, O. & Sparks, R.S.J. (2005). Controls on conduit magma flow dynamics  
379 during lava dome building eruptions. *J Geophys Res* **110**, B02209  
380

381 Murphy, M.D. , Sparks, R.S.J., Barclay, J., Carroll, M.R., Lejeune, A.-M., Brewer,  
382 T.S., Macdonald, R., Black, S. & Young, S. (1998). The role of magma mixing in  
383 triggering the current eruption of the Soufrière Hills volcano, Montserrat, West Indies.  
384 *Geophys Res Letters* **25**, 3433-3436  
385

386 Murphy, M.D., Sparks, R.S.J., Barclay, J., Carroll, M.R. & Brewer, T.S. (2000).  
387 Remobilization of andesite magma by intrusion of mafic magma at the Soufrière Hills  
388 Volcano, Montserrat, West Indies. *J Petrol* **41**, 21-42  
389

390 Reubi, O. & Blundy, J. (2008). Assimilation of plutonic roots, formation of high-K  
391 'exotic' melt inclusions and genesis of andesitic magmas at Volcano de Colima,  
392 Mexico. *J Petrol* **49**, 2221-2243  
393

394 Rutherford, M.J. & Devine, J.D. (2003). Magmatic conditions and magma ascent as  
395 indicated by hornblende phase equilibria and reactions in the 1995-2002 Soufrière  
396 Hills magma. *J Petrol* **44**, 1433-1454  
397

398 Saito, G., Uto, L., Kazahaya, KK., Shinohara, H., Kawanabe, Y. & Satoh, H. (2005).  
399 Petrological characteristics and volatile content of magma from the 2000 eruption of  
400 Miyakejima Volcano, Japan. *Bull Volcanol* **67**, 268-280  
401

402 Sisson, T.W. & Layne, G.D. (1993). H<sub>2</sub>O in basalt and basaltic andesite glass  
403 inclusions from four subduction-related volcanoes. *Earth Plan Sci Letts* **117**, 619-635  
404

405 Sparks, R.S.J., Sigurdsson, H. & Wilson, L. (1977). Magma mixing: a mechanism for  
406 triggering acid explosive eruptions. *Nature* **267**, 315-318  
407

408 Van der Laan, S., Zhang, Y., Kennedy, A.K. & Wyllie, P.J. (1994). Comparison of  
409 element and isotope diffusion of K and Ca in multicomponent silicate melts. *Earth*  
410 *Plan Sci Letts* **123**, 155-166  
411

412 Wager, L.R. & Bailey, E.B. (1953). Basic magma chilled against acid magma. *Nature*  
413 **172**, 68-69

414

415 Wallace, P.J., Anderson, A.T. & Davis, A.M. (1995). Quantification of pre-eruptive  
416 exsolved gas contents in silicic magmas. *Nature* **377**, 612-616

417

418 Yoder, H.S. (1973). Contemporaneous basaltic and rhyolitic magmas. *Amer Mineral*  
419 **58**, 153-171

420

## 421 **Figures**

### 422 Figure 1

423 Compositions of melt inclusions, matrix glasses and mafic inclusion residual glasses.

424 Melt inclusions (diamonds) and matrix glasses (circles) are divided into high-K (open  
425 symbols) and low-K (filled symbols) compositions. Crosses represent mafic inclusion

426 glasses. Grey symbols represent previously published glasses from Soufrière Hills

427 (pluses, *Edmonds et al.*, 2001, 2002; squares, *Harford et al.*, 2003; triangles, *Buckley*

428 *et al.*, 2006). Grey dashes: glasses in hornblende breakdown rims (*Buckley et al.*,

429 2006). Large arrows indicate the schematic effects of hornblende breakdown reactions

430 (reactions 2 and 3, *Buckley et al.*, 2006), or the effect of 5% post-entrapment

431 crystallisation of plagioclase (pl).

432

### 433 Figure 2

434 Decoupled compositional variations in K<sub>2</sub>O and TiO<sub>2</sub> for all glasses. Thick grey

435 arrows indicate how diffusive contamination of K<sub>2</sub>O affects melt compositions. TiO<sub>2</sub>

436 is unaffected because of its very low diffusivity. Symbols as for figure 1.

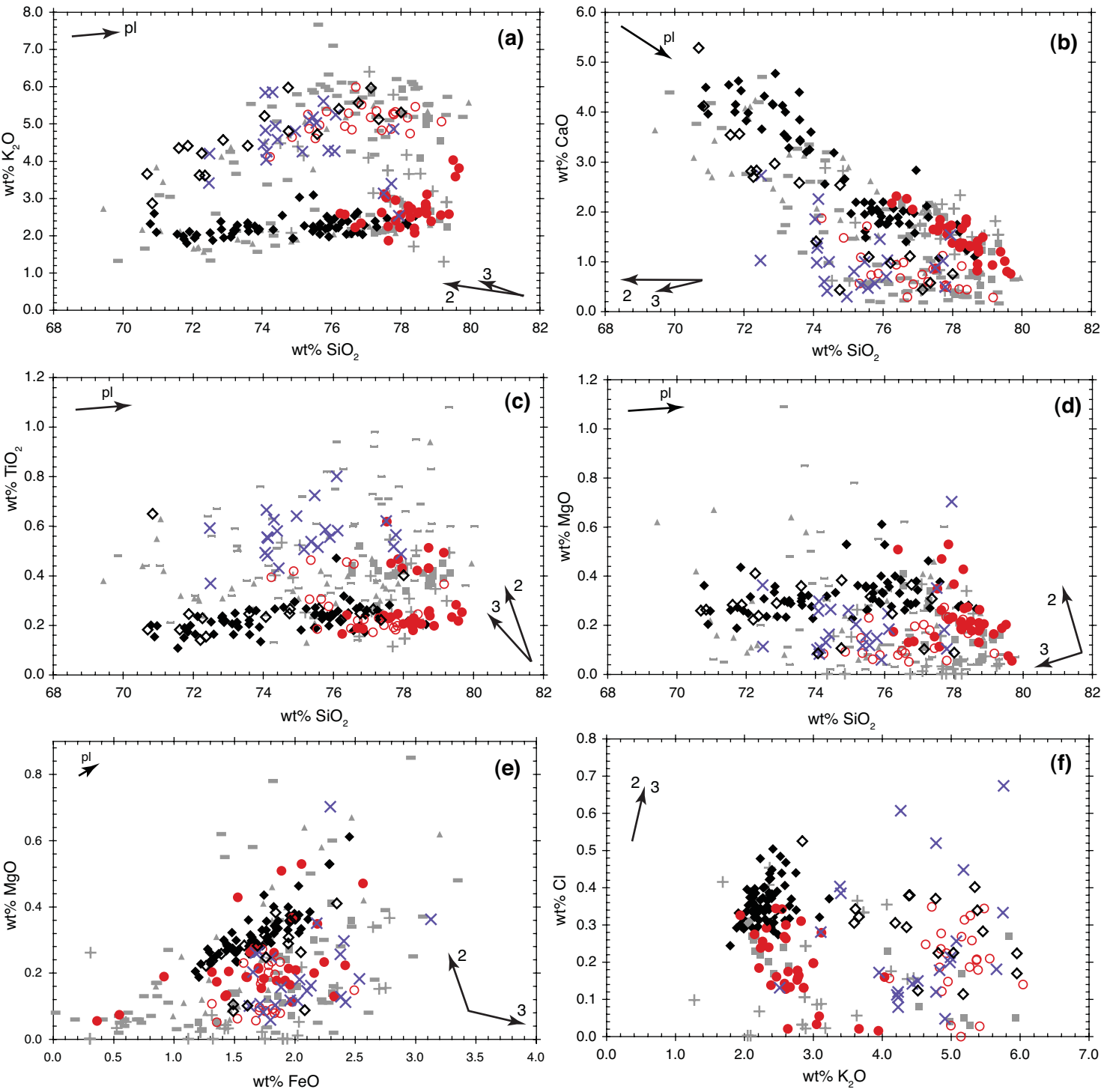


Figure 1

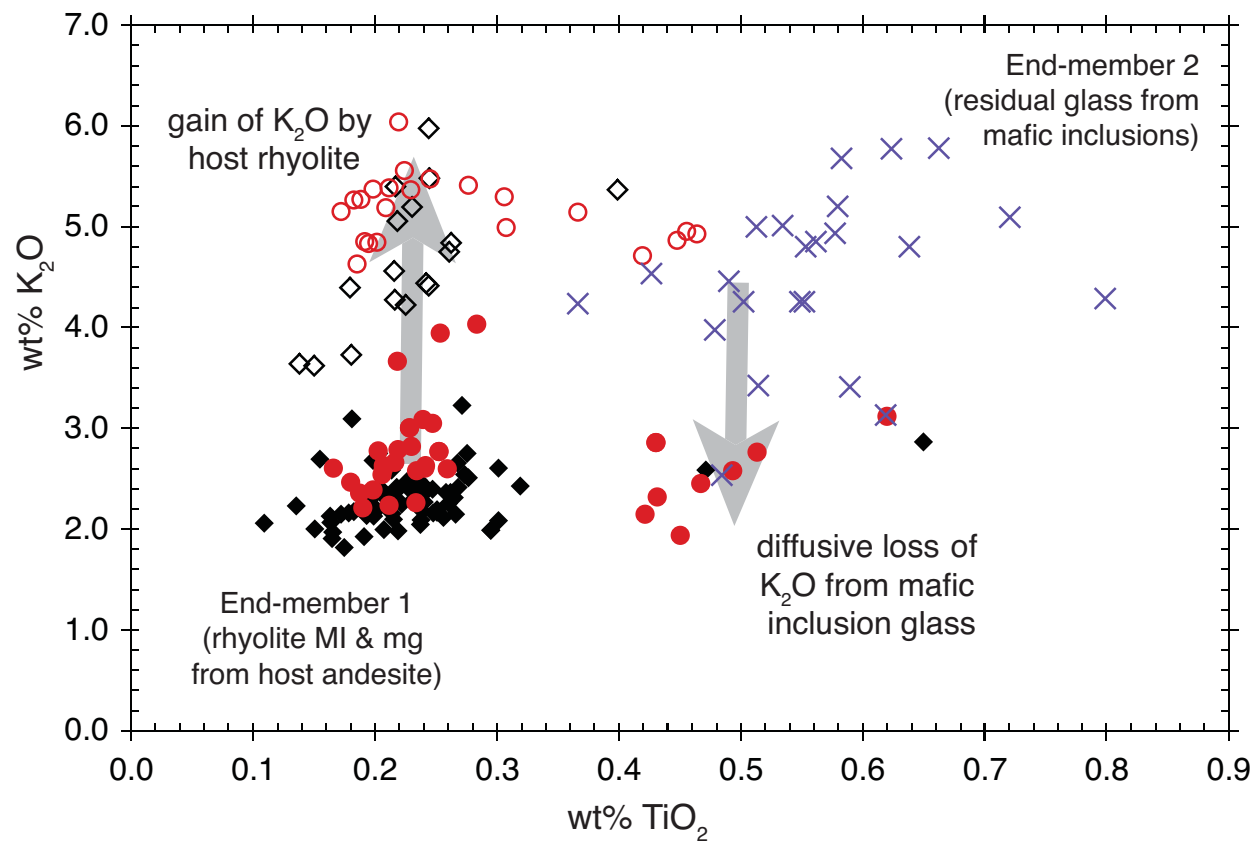


Figure 2